TWO-STEP PLASMA TEXTURING PROCESS FOR INDUSTRIAL SOLAR CELL MANUFACTURING

J. Seiffe, B. Bremen, S. Rappl, M. Hofmann, and J. Rentsch
Fraunhofer Institute for Solar Energy Systems (ISE)
Heidenhofstrasse 2, D-79110 Freiburg, Germany
Tel: +49-761-4588-5499, email: johannes.seiffe@ise.fraunhofer.de

ABSTRACT: This study describes the development of a two-step SF_6/O_2 texturing process using an inline industrial-type plasma system with combined microwave and radiofrequency excitation. It is shown that efficient texturing of polished (100), (111) and multicrystalline surfaces is possible. Multicrystalline silicon solar cells are processed proving an average efficiency gain of 0.2 % absolute compared to standard acidic texturing. With an improved surface passivation even a gain of 0.4 % absolute is achieved.

Keywords: Texturisation, Optical Properties, Solar Cell

1 INTRODUCTION

Since 1998, SF_6/O_2 plasma etching is proposed as alternative surface texturing process in crystalline silicon photovoltaics [1-8]. The possibility to form structures independently of the crystallographic surface orientation makes plasma texturing especially interesting for multicrystalline solar cells. However, for innovative cell concepts requiring a polished rear surface, the single-sidedness of plasma processes as well as the possibility to reach a light-trapping texture from a polished surface with a low silicon removal can be very attractive for monocrystalline cells, too. An effective single-sided and crystallographically independent process could simplify production of rear-side passivated solar cells, introduction of thinner wafers, kerf-loss-free wafering techniques, and usage of casted multicrystalline or mono-like material. Due to the complexity of the SF_6/O_2-plasma reaction with a silicon surface, it is still a challenge to manage a plasma-texturing process in a mass-production feasible plasma tool. It has already been shown that the linear-microwave-antenna excitation (2.45 GHz) of a Roth&Rau SiNA with an additionally in-coupled RF field (13.56 MHz) can be used for inline-feasible plasma texturing processes [9]. We present now a promising two-step SF_6/O_2 texturing process in this high-throughput tool, which is applicable for industrial solar cell manufacturing. Applying this two-step approach, allows the use of a plasma texture without the need of severe changes in the solar cell production processes.

2 EXPERIMENTAL

2.1 Two-step plasma texturing process

We have developed a plasma texturing process for saw-damage free surfaces using SF_6 and O_2 as reaction gases. In Figure 1 the two steps are depicted schematically and by SEM images of prior shiny etched surfaces with (100) and (111) orientation. In the first step, single deep holes are etched in the initial surface forming a pre-structure for the actual texturing. In the second step, the holes are widened resulting in pyramid-like structures. This second step is not independent from the crystallographic orientation. Therefore, cascaded structures occur at the slower etched (111) surface. As can be seen, the process leads to structures, which seem to be reasonably mechanically stable to withstand further processing steps like screen-printing of contacts. Furthermore, it does not show very deep holes or fine roughness, which could be difficult to reach with the deposition of a passivating anti-reflection coating.

The reflection resulting from this process is plotted spectrally resolved in Figure 2 for a (100)-surface, a (111)-surface and for a multicrystalline surface, which was polished in KOH solution prior to the plasma-texturing process. For comparison, reflection values of a shiny-etched surface, of an acidic textured (isotextured) multicrystalline surface and of an alkaline-textured random-pyramid surface are plotted. It can be seen that on
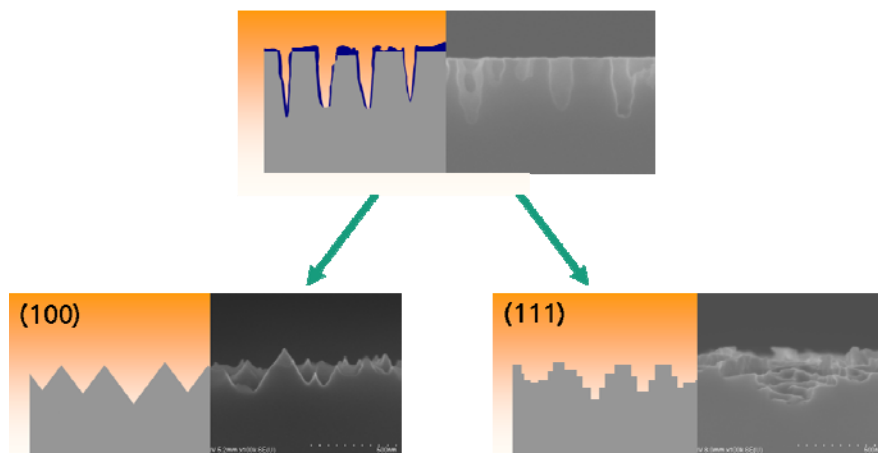
Figure 1: Sketch of the two-step process using deep-etching of single holes in a first step and a crystal-dependent etching of pyramid-like structures on (100)-surfaces and cascaded basins on (111)-surfaces.
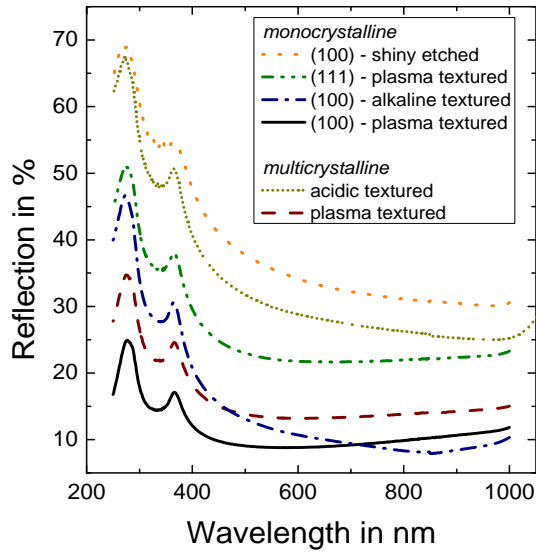
Figure 2: Spectrally resolved reflection of the two-step process on different crystallographic orientations.

(100)-surfaces using the two-step process, reflection values comparable to the alkaline random-pyramid texturing could be achieved. On (111)-surfaces the resulting texturing leads to higher reflection values, but still clearly lower than reflection from the polished surface. Therefore, for the multicrystalline surface a much lower reflection compared to a typical acidic texturing is achieved.

2.2 Solar cells

To evaluate the impact of the developed two-step surface texturing process on final device level, first solar cells have been processed using multicrystalline silicon wafers (p-type, $\rho = 1.5\,\Omega\,cm$, $156 \times 156\,mm^2$, $W = 200\,\mu m$). Three different wet-chemical processes for saw-damage removal before plasma texturing have been performed, as depicted in Figure 3. For one group, the same acidic texturing as performed on the standard reference group has been used as basis for an additional plasma texturing. Further on, the plasma texturing was applied on rather flat surfaces achieved by alkaline polishing in KOH as well as acidic polishing in HF-HNO$_3$. After the different pretreatments, the two-step plasma texturing process was performed on all groups except the standard reference group. The acidic polished wafers
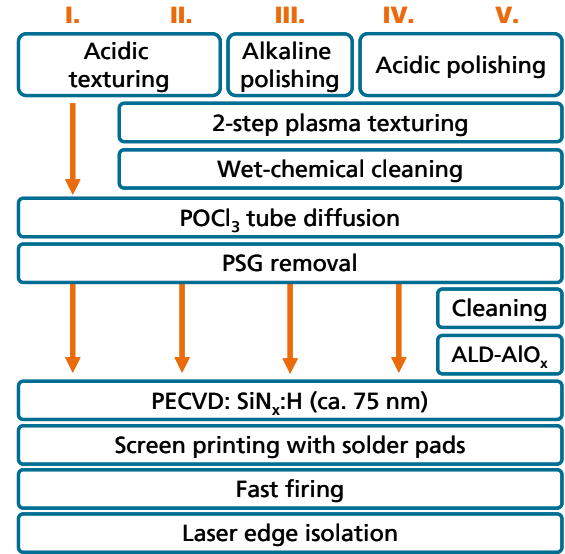

Figure 3: Process flow chart to evaluate solar cells using the two-step plasma texturing approach.

were further split in two groups, one of which received an additional thin Al$_2$O$_3$ layer, deposited by atomic layer deposition (ALD) below the silicon-nitride anti-reflection coating (SiN$_x$-ARC) to improve the front surface passivation. Besides texturing and Al$_2$O$_3$ deposition, the solar cells were processed like industrial standard solar cells (see Figure 3): a POCl$_3$-diffused phosphorous emitter with a sheet resistance of $R_{sh,e} = 65\,\Omega/sq$, PSG removal in diluted HF, SiN$_x$-ARC deposited by PECVD, screen-printed Ag contact fingers on the front and screen-printed Ag/Al solder pads as well as a full Al contact on the rear side, fast firing for contact and Al-BSF formation and edge isolation by a laser groove. For the experiment, neighboring wafers have been taken from one ingot and randomized. In each group, 12 wafers were processed. To optimize the front contact scheme, a variation of three firing peak temperatures has been performed. Finally, the average results of four solar cells per group are compared to evaluate the different processes.

3 RESULTS

In Figure 4, $J(V)$ measurement results for the differ-
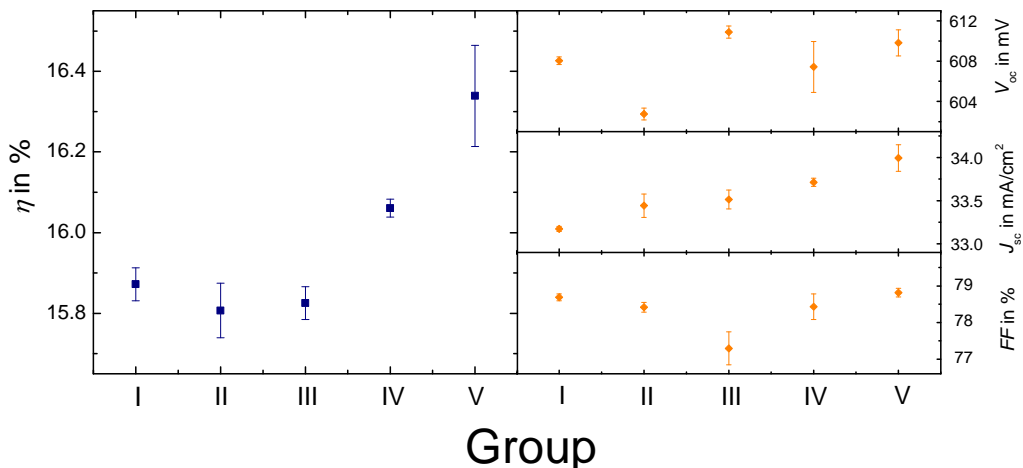
Figure 4: IV results (average and standard deviation of 4 cells). Group numbers correspond to Fig. 3.
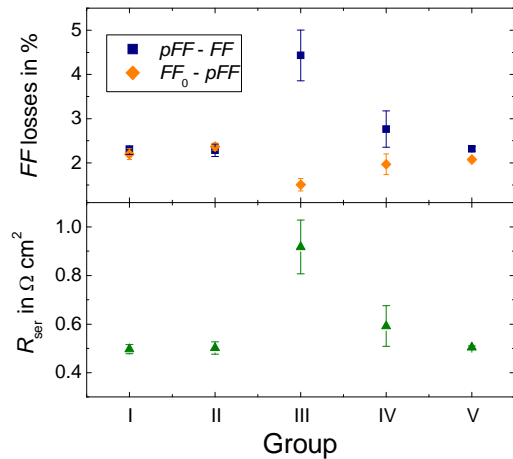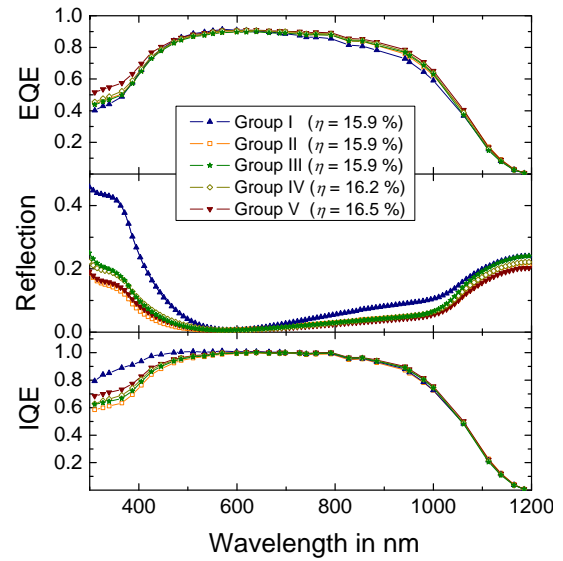
Figure 5: Analysis of fill factor losses. Group numbers correspond to Fig. 3.

Figure 6: EQE/IQE results (best solar cell per group). Group numbers correspond to Fig. 3.

ent groups are summarized. As can be seen for group IV and V an improved conversion efficiency compared to the standard reference (group I) could be achieved. This shows that the acidic polishing process was most suitable as wet-chemical saw-damage removal before plasma texturing. For the combination of acidic texturing and plasma texturing (group II), the open-circuit voltage is clearly decreased compared to the other groups. Most likely, a too rough surface results from this texturing combination afflicting the surface passivation. All further groups show similar open-circuit voltages proving the comparability of surface passivation on plasma-textured surfaces and acidic textured surfaces.

The fill factor is similar to the reference for all plasma-textured groups besides the previously alkaline etched cells (group III). Figure 5 shows an itemization of the fill factor losses in losses due to non-ideality of the diode ($FF_0 - pFF$) and losses due to series resistance ($pFF - FF$). Additionally, the series resistance R_{ser} determined from the comparison of the light and dark $J(V)$ characteristic is plotted. It can be seen that the cells of group III have a significantly higher series resistance leading to the observed loss in fill factor.
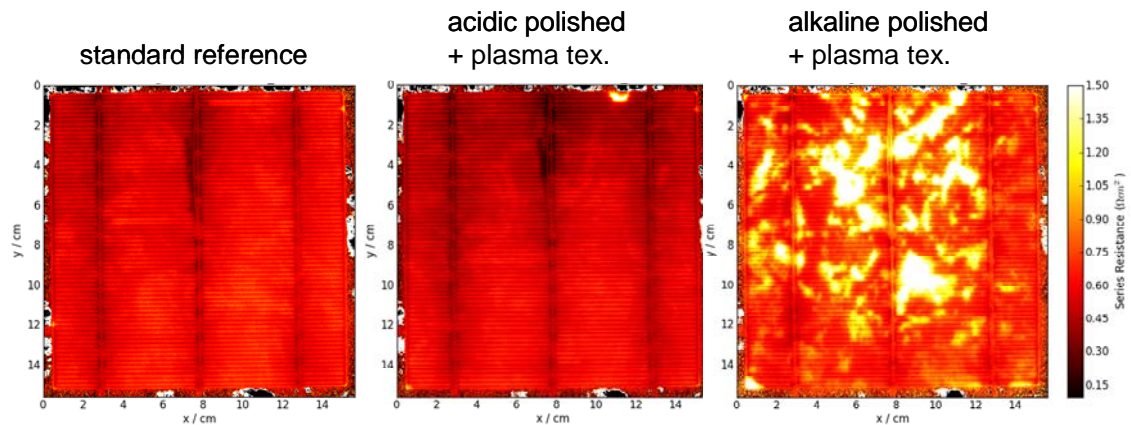
The series resistance mapping in Figure 7 shows that the problem appears especially on single grains. It might be that varying surface reflections on the grains result in different reactions on the radiation heaters in the firing

process. Therefore, the optimal temperature condition cannot be achieved for all grains at once. A similar problem is already described for alkaline texturing on multicrystalline surfaces [10]. Moreover, etch rates depending on the different surface orientations could lead to step formation between the grains, which might complicate a homogeneous screen-printing.

The efficiency improvement of the plasma-textured cells in group IV and V is based on an increased short-circuit current density J_{sc}. Figure 6 shows the external quantum efficiency (EQE), the reflection, and the thereof calculated internal quantum efficiency (IQE) for the champion cell of each group. It can be seen in the EQE that the gain in J_{sc} for the plasma-textured cells comes from the front side (short wavelengths) as well as from the rear side (long wavelengths). The reflection curves show that this benefit is achieved by an improved light trapping by the plasma-textured cells compared to the standard acidic textured ones. However, regarding the IQE, it can be seen that the reference group is clearly superior in the short-wave range. The reduced IQE does not seem to have origin in a lack of surface passivation as in this case also the open-circuit voltage should be afflicted. Furthermore, the fact that the loss of quantum efficiency

Figure 7: Series resistance mapping.

reaches up to about 600 nm indicates an emitter problem. As already known for alkaline-etched pyramid-like textures, the phosphorous diffusion on peaks is much more pronounced as the phosphorous diffusion in troughs [11]. This can be easily understood as the diffusion takes place from different surfaces simultaneously to the peak. As the pyramids observed for the plasma texturing are in the range of the phosphorous emitter depth, it is to assume that the pyramids are almost completely converted to n-type. Additionally, a main part is doped considerably higher, since it is reached by the phosphorous diffused from different pyramid surfaces. The higher doping level however leads to shorter minority charge carrier diffusion lengths and reduces the collection probability for these carriers. The main disadvantage of the small pyramids is that the density of peaks is much higher and therefore also the regions with lower collection probability are increased. It is to assume that this effect leads to the lower IQE observed for the plasma-textured solar cells. To further improve the solar cells, it is aimed to increase pyramid scales by optimizing the plasma-texturing process and to adapt the emitter diffusion process to achieve lower phosphorus surface concentration in the small pyramids. An IQE comparable to standard acidic textured cells combined with the low reflectance by the plasma texturing would result in an additional short-circuit current gain of even ca. 1 mA/cm^2.

4 SUMMARY AND CONCLUSIONS

Silicon solar cells based on multicrystalline substrate wafers, were produced as proof of concept for the developed two-step plasma-texturing process. An average efficiency improvement of 0.2 % absolute compared to standard solar cells was achieved by just exchanging the surface texturing process. With an additional Al_2O_3 layer below the silicon nitride to improve the passivation of the plasma-textured surface the conversion efficiency was improved in average by 0.4 % absolute.

Spectral-response measurements show that a significant part of the benefit due to the reduced reflection is lost by lower internal quantum efficiency (IQE). The decreased IQE is supposed to result from a low effective minority-carrier diffusion length in the emitter. Due to the small sizes, the phosphorus diffusion leads to high doping inside the pyramid-like structures and thus to a lower collection probability of charge carriers generated inside the texture. Increasing the structure sizes and adapting the emitter diffusion to the plasma texturing are the main objectives for future development. As this first test was only a proof of concept without any adaption of the different processes to the two-step plasma texturing process, it is to assume that a more pronounced efficiency improvement is possible.

5 ACKNOWLEDGMENTS

6 REFERENCES

[1] D. S. Ruby, P. Yang, S. Zaidi, S. Brueck, M. Roy, and S. Narayanan, "Plasma etching, texturing, and passivation of silicon solar cells," presented at NCPV Photovoltaics Program Review. 15th Conference, Denver, CO, USA, 1998.

[2] R. Lüdemann, B. M. Damiani, A. Rohatgi, and G. Willeke, "Silicon solar cells with black silicon texturization," presented at Proceedings of the 17th European Photovoltaic Solar Energy Conference, Munich, Germany, 2001.

[3] H. F. W. Dekkers, G. Agostinelli, D. Dehertoghe, and G. Beaucarne, "Improved performances of mc-Si solar cells by isotropic plasma texturing," presented at Proceedings of the 19th European Photovoltaic Solar Energy Conference, Paris, France, 2004.

[4] J. Rentsch, N. Kohn, F. Bamberg, K. Roth, S. Peters, R. Lüdemann, and R. Preu, "Isotropic plasma texturing of mc-si for industrial solar cell fabrication," presented at Proceedings of the 31st IEEE Photovoltaic Specialists Conference, Orlando, Florida, 2005.

[5] J. Yoo, K. Kim, M. Thamilselvan, N. Lakshminarayn, Y. K. Kim, J. Lee, K. J. Yoo, and J. Yi, "RIE texturing optimization for thin c-Si solar cells in SF 6 /O 2 plasma," *Journal of Physics D: Applied Physics*, vol. 41, pp. 125205, 2008.

[6] M. Moreno, D. Daineka, and P. Roca i Cabarrocas, "Plasma texturing for silicon solar cells: From pyramids to inverted pyramids-like structures," *Solar Energy Materials and Solar Cells*, vol. 94, pp. 733-737, 2010.

[7] J.-M. Shim, H.-W. Lee, and K.-Y. Cho, "17.6% Conversion Efficiency Multicrystalline Silicon Solar Cells Using the Reactive Ion Etching with the Damage Removal Etching," *International Journal of Photoenergy*, vol. 2012, 2012.

[8] B. T. Chan, E. Kunnen, K. Xu, W. Boullart, and J. Poortmans, "Two-Step Plasma-Texturing Process for Multicrystalline Silicon Solar Cells With Linear Microwave Plasma Sources," *IEEE Journal of Photovoltaics*, vol. 3, pp. 152, 2013.

[9] P. Piechulla, J. Seiffe, M. Hofmann, J. Rentsch, and R. Preu, "Increased ion energies for texturing in a high-throughput plasma tool," presented at Proceedings of the 26th European Photovoltaic Solar Energy Conference and Exhibition, Hamburg, Germany, 2011.

[10] B. Rounsaville, I. B. Cooper, K. Tate, M. Kadish, A. Das, and A. Rohatgi, "Analysis of cast mono-crystalline ingot characteristics with applications to solar cells," presented at Proceedings of the 38th IEEE Photovoltaic Specialists Conference, Austin, TX, USA, 2012.

[11] H. Wagner, S. Steingrube, B. Wolpensinger, A. Dastgheib-Shirazi, R. Chen, S. T. Dunham, and P. P. Altermatt, "Analyzing emitter dopant inhomogeneities at textured Si surfaces by using 3D process and device simulations in combination with SEM imaging," presented at Proceedings of the 38th IEEE Photovoltaic Specialists Conference Austin, TX, USA, 2012.